# The Meso-NH Atmospheric Simulation System as a Research Tool at Mesoscale

J.P. Lafore, V. Ducrocq, P. Bougeault*, A. Diongue,
P. Jabouille, G. Jaubert, I. Mallet, D. Ricard and J. Stein

CNRM/GMME (Météo-France and CNRS)
* ECMWF

## 1. The Meso-NH model

The Meso-NH Atmospheric Simulation System is a joint development of Météo-France and Laboratoire d'Aérologie. It comprises several elements; a non-hydrostatic numerical model able to simulate the atmospheric motions, ranging from turbulent large eddies to the synoptic scale, with a comprehensive physical package, a flexible file manager, an ensemble of facilities to prepare initial states, either idealized or interpolated from meteorological analyses or forecasts, a post-processing and graphical facilities to visualize the results, and an ensemble of interactive procedures to control theses functions. Among the distinctive features of this ensemble we should notice that the current formulation of Meso-NH allows for the use of three anelastic systems: the *Lipps and Hemler* (1982) system, the traditional one of *Wilhelmson and Ogura* (1972) and a simplified implementation of the pseudo-incompressible system of Durran (1989). It is also important to note that Meso-NH has been designed and developed as a **research tool** and not as a forecast system at small scales as this mission is devoted to the ARPEGE-IFS / ALADIN couple at Météo-France. The details of the model dynamics can be found in Lafore et al (1998). Only a brief summary is given here.

### *a. General description*

The general equations of the model are written on the conformal plane in order to take into account the Earth's sphericity. The inclusion of orography is achieved by using the Gal-Chen and Sommerville (1975) vertical coordinate. The flux form of the equations has been preserved by considering covariant and contravariant components of the velocity (*Viviand*, 1974). The model equations are written for the following prognostic quantities: momentum $\rho_d\vec{u}$, dry potential temperature $\vartheta$, mixing ratios $r_n$ of the different water phases, turbulent kinetic energy *TKE.* $\rho_d\vec{u}$ stands for the dry density of the reference state used to separate the thermodynamic variables into a horizontally uniform hydrostatic reference state and a variable perturbation. The pressure perturbation is determined by solving an elliptic equation obtained by enforcing the anelastic continuity equation. This elliptic equation is solved by a Richardson method where preconditioning is achieved by solving the same problem without the inclusion of orography. The temporal numerical scheme consists of a purely explicit leap-frog scheme with a weak time filter (*Asselin,* 1972) applied to control the numerical mode growth. The spatial discretization is a standard second-order accurate centred difference. In order to prevent the accumulation of energy at the 2 $\Delta x$ scales, a fourth-order numerical diffusion is applied to all prognostic equations after subtracting their corresponding large scale field. The upper boundary condition is a rigid lid associated with a sponge layer to prevent reflection from the top. Several formulations for the lateral boundary conditions are available; cyclic, rigid-wall, externally forced or radiative open conditions.

The model uses a comprehensive physical package to reproduce the different atmospheric processes: turbulent and convective motions, radiation, soil/atmosphere exchanges, and phase changes of water. It also includes an inline chemical module allowing its use for environmental studies. The turbulence scheme is based on a one and half order closure formulation in which the mixing coefficient is computed by using the prognostic *TKE* (*Redelsperger and Sommeria*, 1981) and the physical mixing length of *Bougeault and Lacarrère* (1989). This scheme, described in *Cuxart* (1997), has been validated in 1D and 3D Large Eddies Simulations experiments. The convection scheme has been adapted from Kain and Fritsch (1990) and has been assessed in a model intercomparison performed with the TOGA-COARE data set (*Bechtold et al.*, 1998). The microphysics is represented by a bulk scheme combining a three classes ice parameterisation to the Kessler's scheme for warm processes (*Pinty and Jabouille*, 1998, *Caniaux at al*, 1994). The radiation scheme is the operational scheme developed at ECMWF (*Morcrette*, 1989). The ISBA soil scheme of *Noilhan and Planton* (1989) has been implemented in the model and validated with the Hapex Mobilhy data set (*Belair et al.*, 1998). A recent improvement concern the development of the Town Energy Budget by *Masson et al.* (2000) to represent fluxes by urban surfaces.

### b. *The two-way interactive grid-nesting*

The two-way interactive grid-nesting (TWN) technique of *Clark and Farley* (1984) has been implemented in Meso-NH to allow one to reach higher resolution in a limited portion of the computation domain. The ratio of temporal and spatial resolution between the coarse mesh model (CM) and the nested fine-mesh models (FM) are constrained to be integers. Interactions between the CM and FM are allowed by two means: a downscale flow, which is achieved by using the CM values as boundary conditions for the FM models, and an upscale flow, which comes from relaxing the CM values towards the FM results in the area where the models overlap. These two interactions allow a strong coupling between the models simulating the dynamics of the atmosphere at different scales and their interactions.

We brought some improvements to the original TWN of *Clark and Farley* (1984), in order to use high resolution ratio between models without spurious reflections at inner boundaries. The downscale exchange of the information is performed by the specification of lateral boundary conditions for all of the prognostic variables. Instead of replacing the FM model lateral boundaries by the CM model values as done by *Clark and Farley* (1984), a radiative equation is used for all type of waves, as tested by *Chen* (1991) for acoustic waves in a nested compressible model. Thus the normal velocity $u_n$ is computed by a modified *Carpenter* (1982) equation. It allows the evacuation of gravity wave energy to avoid reflection at the lateral boundaries. Note that this is formally the same equation as for the outermost model:

$$\frac{\partial u_n}{\partial t} = \left(\frac{\partial u_n}{\partial t}\right)_{LS} - C\left(\frac{\partial u_n}{\partial x} - \left(\frac{\partial u_n}{\partial x}\right)_{LS}\right) - K\left(u_n - u_{nLS}\right)$$

where $C = u + C^*$ is the sum of the interior velocity and a fixed phase velocity $C^*$ and $K$ the inverse of a damping time. The LS subscript stands for Large Scale field which is obtained by the interpolation of the CM model field at the boundary of the FM model at every time-step. The Bikhardt algorithm, which is employed for the horizontal interpolation, uses 4 points in each horizontal direction and a linear vertical interpolation is used to correct the changes between the CM and FM orography. The other prognostic FM variables are either spatially interpolated at the FM boundary from their large-scale CM values, or extrapolated from FM interior grid points in the case of inflow or outflow respectively.

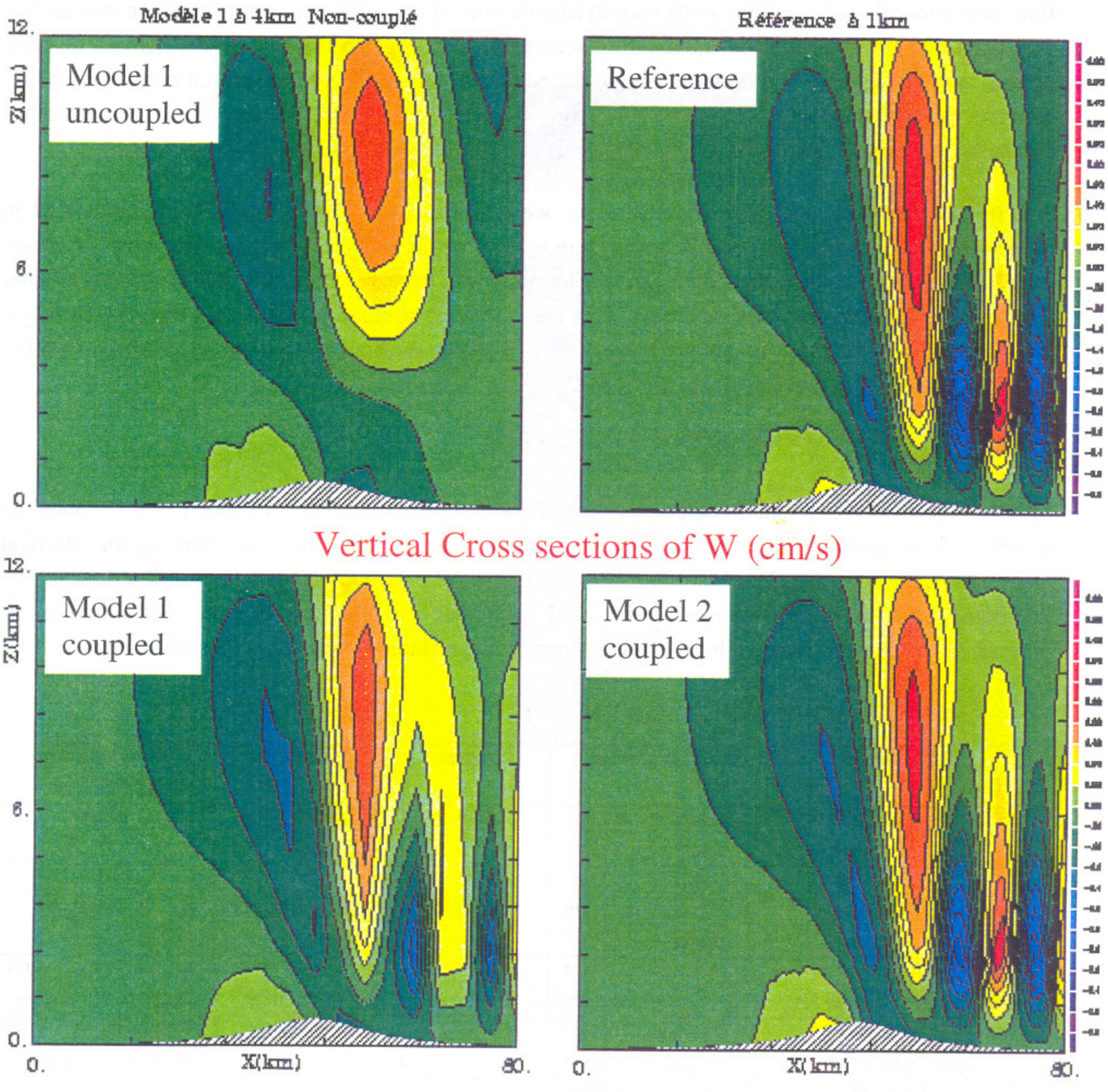


Figure 1: Vertical cross section of the vertical velocity (cm/s) for the trapped lee-waves case of Durran (1995 )on the model 2 domain for: (a) model 1 (4 km resolution) without nesting, (b) the reference simulation at 1 km resolution, (c) model 1 with the two-way interactive gridnesting and (d) model 2 (1 km resolution).

The upscale exchange of information is performed by adding a tendency term to all of the CM model prognostic equations except for *TKE*:

$$\frac{\partial \alpha}{\partial t} = S_{\alpha} - \frac{\alpha - \alpha_{ss}}{\tau}$$

where $t$ is a relaxation time equal to four time steps of the CM model and $a_{SS}$ is the average of the field values over all of the FM grid points included in the CM grid. No vertical interpolation is needed because the average of the FM orography is equal to the CM orography. This method of transferring information from the small scales towards the large scale allows the CM model the freedom to include this "sub-gridscale information" in its own dynamics: for instance, the pressure term in the momentum will react and transfer the local momentum sources or sinks due to the FM model (waves, diabatic effects...) into the whole CM domain. The so-called fast terms that govern the saturation processes will interpret this information as a new sub-gridscale source for the diabatic process (i.e. a supplementary convection scheme if, for instance, the FM model is able to explicitly resolve the convection).

Among the numerous idealized and real cases we performed to validate the TWN implemented in Meso-NH, Fig. 1 presents the result for a severe test corresponding to 2D trapped lee-waves (*Durran*, 1995). Model 1 has a too crude horizontal resolution (4 km) to represent the lee-waves, whereas model 2 at 1 km resolution retrieves the solution of the reference simulation performed on a much larger domain. Only TWN allows to get the right solution, whereas spurious reflections are obtained with the one-way nesting with this resolution ratio.

### c. *Some additional features et remarks*

Méso-NH have been designed to answer to the needs of a large research community. For instance the model may be used in 2D or even 1D form, which is very useful for understanding the physical processes involved in the simulations or to test and improve parametrisation schemes. It allows for in-line computation of the full budget of all model prognostic variables over domains and time periods prescribed by the user. It also allows for the transport and turbulent diffusion of passive scalars.

| **Case study** | **Resolution** | **Duration** | **Initial fields** | **Initialisation procedure** |
|---|---|---|---|---|
| 26 Dec 99<br>Christmas Storm | model 1: 40 km<br>model 2: 10 km | 24 h<br>12 h | Météo-France<br>4Dvar | none |
| 12-13 Nov 99<br>Aude flash flood | model 1: 10 km<br>model 2: 2.5 km<br>model 3: 1.25 km | 18 h<br>18 h<br>3 h | Météo-France | none |
| 4 Aug 94<br>Ile de France Squall line | model 2: 2.5 km<br>and 1.25 km | 4 h | Météo-France | Surface data: OI<br>Radar + IR: Boggus |
| 13-14 oct 95<br>Cévennes-Vivarais | model 1: 10 km<br>model 2: 2.5 km | | Météo-France | Surface data: OI<br>Radar + IR: Boggus |
| 19 Sep 99<br>MAP: Foehn | model 1: 40 km<br>model 2: 10 km<br>model 3: 2.5 km | 48 h | Météo-France | none |
| 21 Aug 1992<br>HAPEX-SAHEL<br>Squall line | model 1: 30 km<br>model 2: 5 km | 18 h | ECMWF<br>ERA | none |

Table 1: Simulations table.

## 2. Some examples of Meso-NH simulations at fine scales

Meso-NH cannot directly contribute to the main object of the present ECMWF Workshop focused on Numerical Methods for Very High Global Models. On the contrary its application in a research mode can help us to answer to the following questions concerning;

- improvements expected at high resolution,
- new problems specific to those scales to be solved: parametrisations, initialisation...
- the predictability at small scales,
- the strategy to develop with the help of similar research tools.

We present in this second part some results of simulations of real cases performed at different resolutions (40 km to 2.5 km) for different types of situations and different latitudes. Table 1 summaries the main characteristics of each case study and the corresponding Meso-NH configuration. We will mainly focus on the convection organisation and on resulting precipitation, as most progresses are excepted in that area where diabatic effects are strong and difficult to be well represented at low resolution.

### *a. Christmas Storm*

*Mallet at al.* (1999) demonstrated for the FASTEX IOP7 the ability of Meso-NH to simulate large scale flow dynamics (70 km resolution) with skills similar to the ones of ECMWF and Météo-France operational models. Owing to the gridnesting technique it is thus possible to correctly simulate the large flow with the first model and small features in the active part of a storm in order to look at the relative contribution of both scales and at their interactions. The Christmas storm brought us an opportunity to test this approach for an extreme event. The main conclusions that we drawn on that case are the following.

(i) The evolution of the surface low simulated by Meso-NH is well located in space (error less than 50 km) with the correct intensity as compared with surface observations (Fig.2) The absolute minimum is reached about 3h later than observed.

(ii) Meso-NH with only one model at 40 km allows to improve the low intensity of ~2 hPa relatively to the ARPEGE forecast.

(iii) A supplementary ~2 hPa improvement is obtained owing to the use of the nesting of a second model at 10 km resolution, and the storm intensification is a little faster.

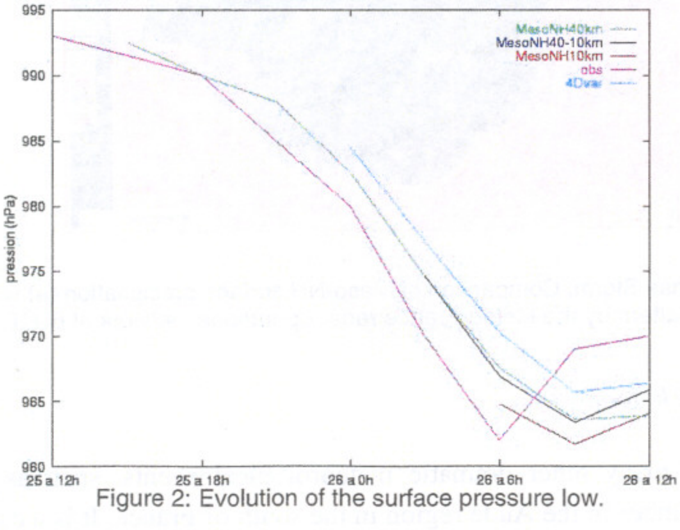


Figure 2: Evolution of the surface pressure low.

(iv) The precipitation pattern is very realistic at large and smaller scale with banded structures similar to the ones observed by the radar network (Fig. 3). Nevertheless no quantitative comparison has been performed at that time.

(v) The strong surface wind is also well reproduced although a little underestimated, possibly due to the fact that gustiness is not included in the model estimation.

In short, for this case of strong large scale forcing, it seems that higher resolution (and better physics?) allows a weak but sensible improvement of the simulation. It also illustrates the efficiency of the two-way interactive gridnesting.

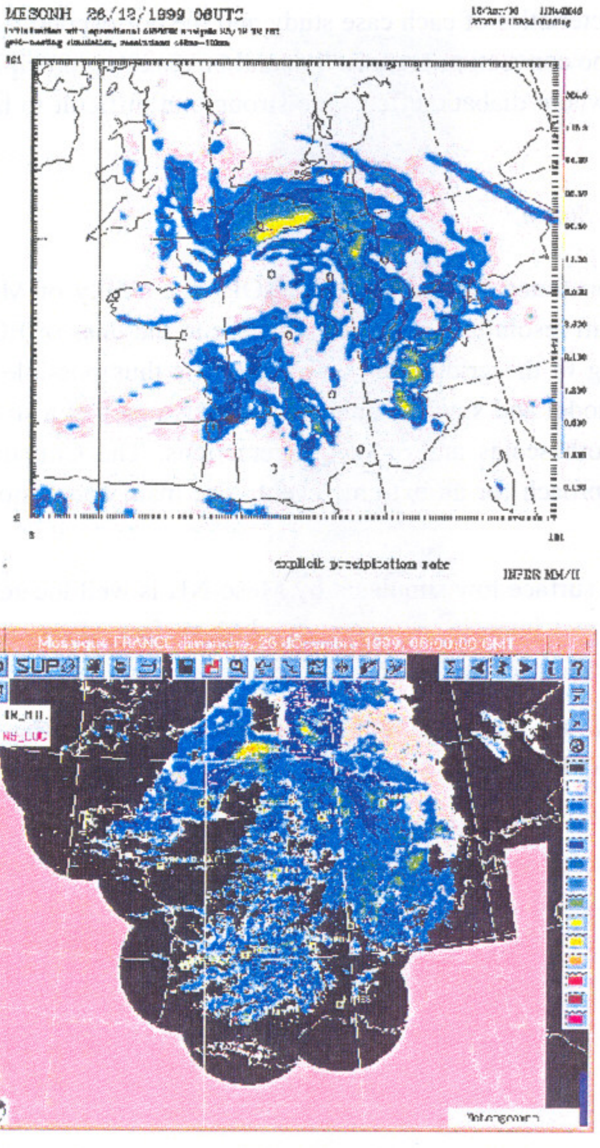


Figure 3: Christmas Storm: Comparison of Meso-NH surface precipitation (a) with observed reflectivity pattern by the Météo-France radar operational network at 6UTC.

*b. Aude flash flood*

The 1999 year brought many other dramatic meteorological events, such as the flash flood that occurred the 12-13 November in the Aude region in the south of France. It is a case strongly forced by the large scale flow that the ARPEGE – ALADIN system forecast correctly. Starting from the Météo-France 3D-Var analysis, Meso-NH also succeeded to simulate that case.

(i) The comparison of surface precipitation with radar reflectivity (Fig. 4) indicates that the 2.5 km resolution allows to reproduce the intense line of convection at the right position and with the correct orientation.

(ii) The maximum of precipitation accumulated over 18 h (Fig. 5) reaches 325 mm at the 2.5 km scale, approaching the absolute maximum observed in the same area (406 mm). The precipitation patterns are similar except precipitation over the Nimes area that Meso-NH failed to reproduced.

(iii) Comparison between the ALADIN forecast and Meso-NH after averaging at the same scale (10 km) shows an improvement for accumulated rain (180 mm and 260 mm for ALADIN and Meso-NH respectively.

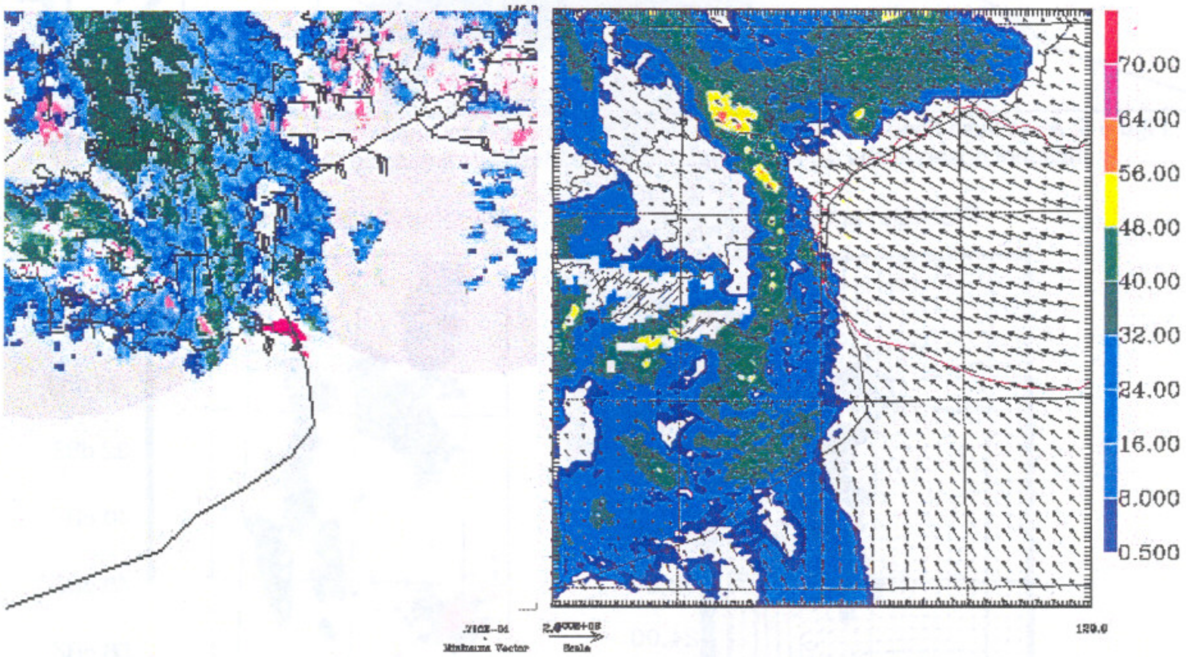


Figure 4: Aude flash flood case: Comparison of Meso-NH surface precipitation (a) with observed reflectivity pattern by the Météo-France radar operational network at 20 UTC.

### c. *Initialisation procedure at small scale*

In the absence of strong large scale forcing, fine scale simulation are often less successful to reproduce convective events when initial states are simple interpolated from meteorological analyses or forecasts. *Ducrocq et al.* (2000) developed a method to introduce in the large scale initial state some information about a given storm. The approach combine optimal interpolation (OI) analysis and bogussing method. The information provided by the Météo-France surface mesonet observations (relative humidity, temperature and winds) is incorporated by means of a mesoscale (OI) analysis. Simple cloud and precipitation analyses based on conventional radar reflectivities and infrared satellite data help to adjust the humidity and hydrometeor fields of the initial state. Thanks to this initialisation procedure, the resulting initial state describes the signature of mesoscale convective systems (MCS).

*Ducrocq et al.* (2000) have shown that the initialisation procedure applied to an observed convective system markedly improves the fine scale model results. Meso-NH succeeds in simulating a convective line observation which compares well with the observations (Fig. 6).

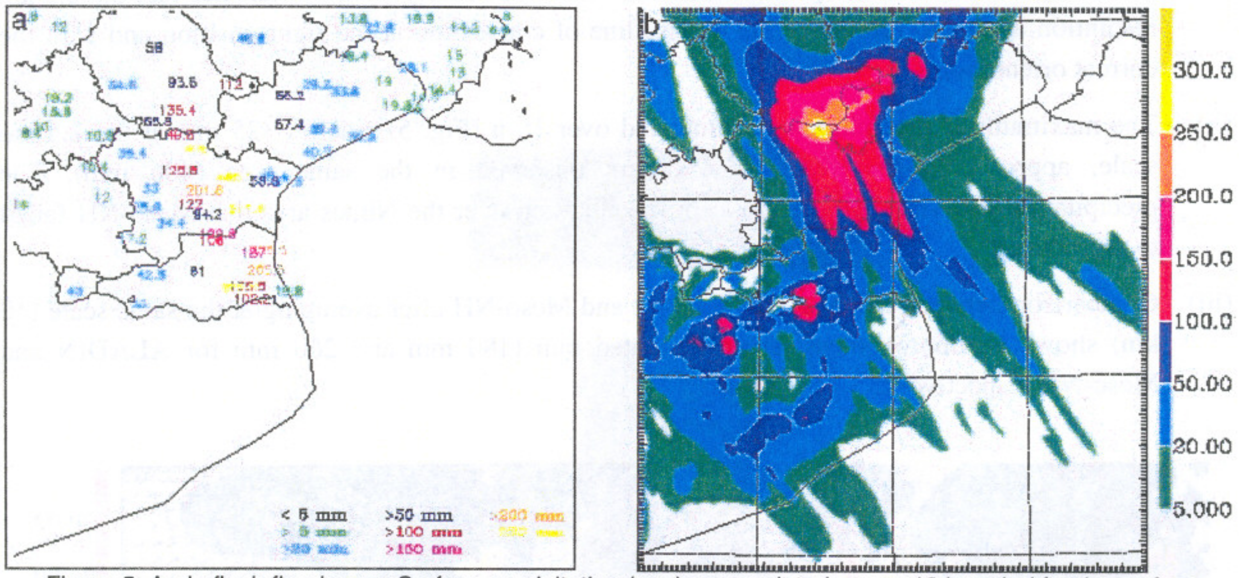


Figure 5: Aude flash flood case: Surface precipitation (mm) accumulated over a 18 h period for the surface mesonet observations (a) as compared with the Meso-NH fine scale (2.5 km) simulation (b).

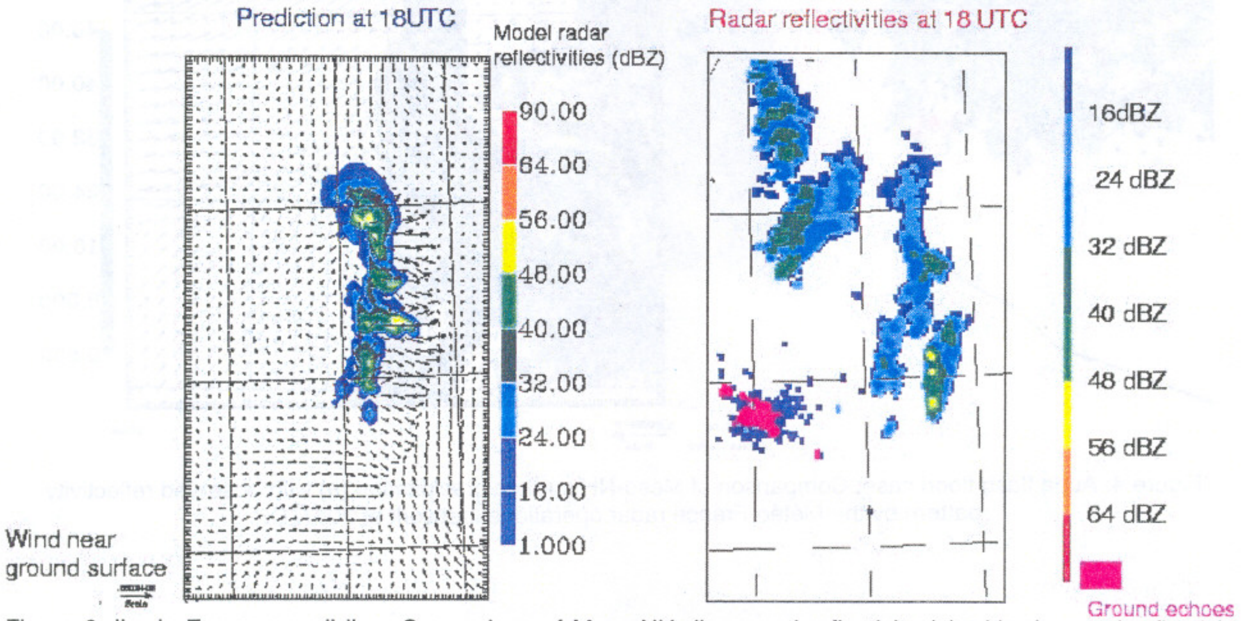


Figure 6: Ile de France squall line: Comparison of Meso-NH diagnosed reflectivity (a) with observed reflectivity pattern by the Météo-France radar operational network at 20 UTC. Simulated surface wind vectors are superposed.

The simulated rainfall are of the same order as those observed (Fig. 7). Sensitivity experiments have proved that both parts (mesoscale analysis and bogus) of the initialisation procedure are necessary at least for this case occurring over a flat terrain region. This method have been successfully applied to other storm cases occurring in the northern part of France.

Recently *Nuret et al.* (2000) incorporated 3D fields of humidity and of wind retrieved from airborne Doppler radar of a MCS observed during the TOGA-COARE experience thanks to an OI analysis.

Méso-NH simulations of this system at 20 km resolution were dramatically improved in term of precipitation and organisation (propagation, associated meso-vortex). Sensitivity experiments suggested that both fields contributed to this result, but the humidity field had the major contribution.

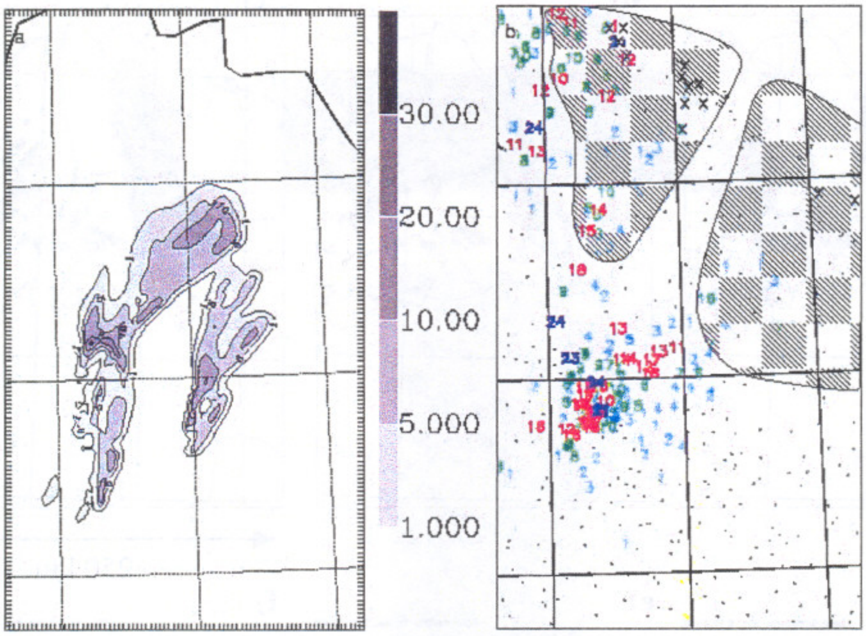


Figure 7 : Ile de France squall line: Meso-NH surface precipitation (mm) accumulated over a 3 h period (a) as compared with the for the surface mesonet observations (b).

### d. *Intense convective events over Cévennes-Vivarais*

In the frame of a French hydrological research program PNRH, Meso-NH is presently used to simulate intense precipitation episodes (more than 100 mm) occurring over the Cévennes-Vivarais relief where radar and a rain gauges network allow a better estimation of the precipitation field. The initialisation procedure of *Ducrocq et al.* (2000) has been used to simulate this type of event such as the one that occurred on the 13-14 Oct 1995, allowing to draw the following main conclusion.

(i) Méso-NH reproduces this convective event at about the right location (~30 km shift to the east), with the same extension and its steady state character (Fig. 8).

(ii) Accumulated precipitation reach a maximum of 100 mm between 1 and 6UTC, to be compared with the 135 mm observed maximum (Fig. 9).

(iii) The assimilation of surface observation was determinant to obtain this improvement, whereas the model was not sensitive to the bogus technique for this and other orographic cases.

### e. *A case of Foehn during the MAP experiment*

The data collected during the MAP experiment are presently treated and extensively analysed owing to the use of Meso-NH both for "wet" and "dry" cases. Figure 10 give an example of such simulation of a Foehn event that occurred on the 19 Sep 1999 in the Rhine valley. The 2.5 km is sufficient to reproduce the wind acceleration and drop that has been observed by the Merlin aircraft. The maximum intensity is a little underestimated possibly due to the low resolution (2.5 km) used for this simulation as compared with the valley size. This case illustrate the potential improvements of high resolution simulations over complex orography.

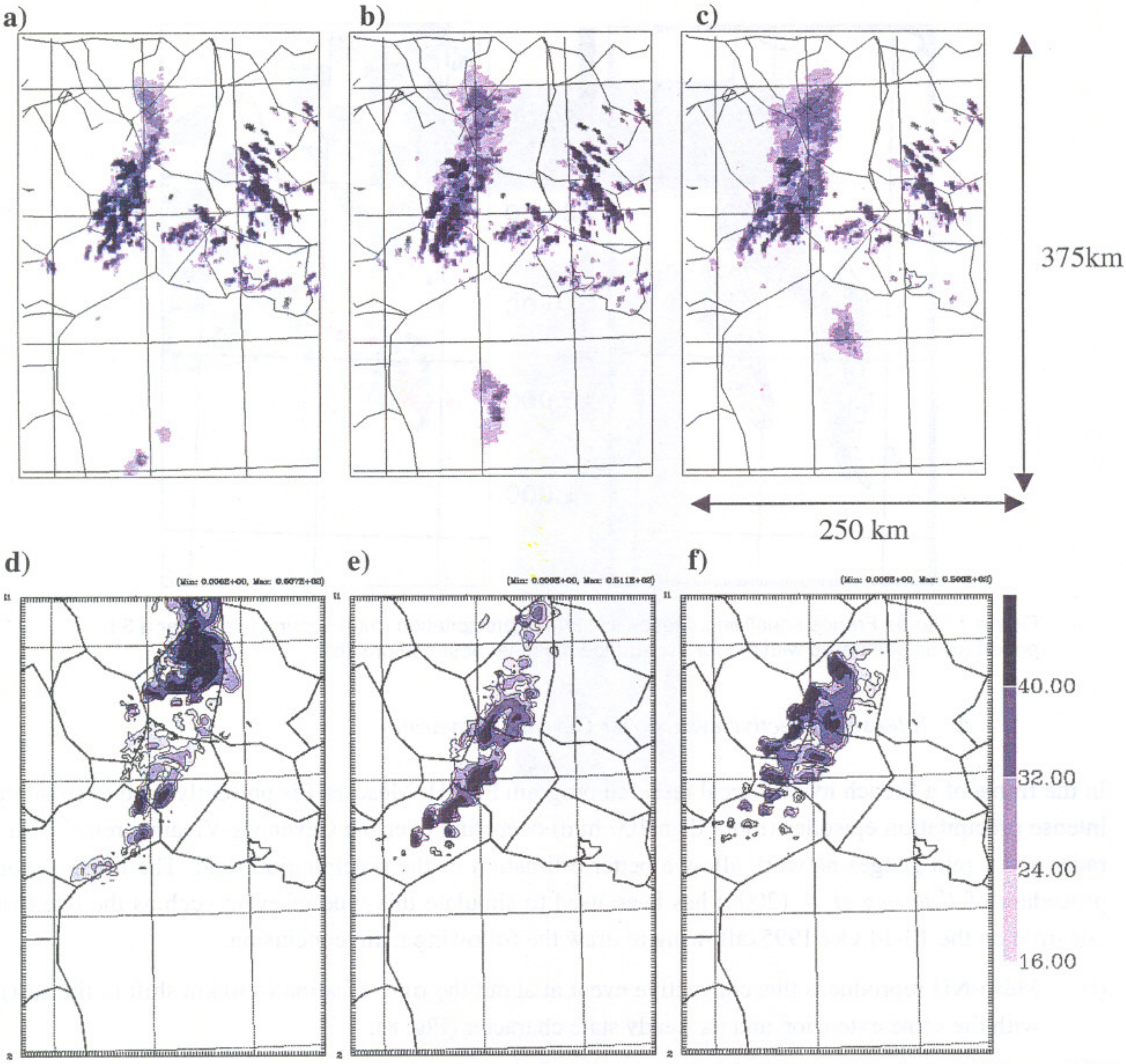


Figure 8: Cévennes-Vivarais case : Reflectivity field (dBz) observed by radar of Nîmes (a : 01 UTC ; b : 0330UTC ; c : 06UTC on the 14/10/95) and Meso-NH diagnosed reflectivity (d : 01 UTC ; e : 0330UTC ; f : 06UTC on the 14/10/95). Radar surface echoes have nor been suppressed.

### *f. Simulation of the triggering and mature stages of an African squall line*

The gain brought by higher resolution is expected to be different for tropical convection than at mid-latitudes where the balanced flow often forces convection. Thanks to resolutions equal and greater than 5 km, the convection can be explicitly represented avoiding thus the use of convection schemes often inaccurate to trigger convection at the right time and location. A current research performed in the frame of the European West African Monsoon Project WAMP illustrates the benefit of high resolution to simulate the life cycle of a squall line observed the 21 Aug 1992 during the HAPEX-Sahel experiment.

(i) 5 km resolution is sufficient to simulate the triggering of the system over the Aïr mountains at 11 h, and the development of an intense fast moving squall line propagating south-westward with main characteristics (speed, temperature drop, precipitation...) similar to observations (Fig. 11).

(ii) The gridnesting is necessary to represent convection occurring to the south and that influences the monsoon flux and the squall line onset.

(iii) Lower resolutions simulation with the convection scheme do not allow to correctly simulate this system. Globally the main defaults of these simulations are a lack of convection during the night and the convective systems triggering in dry regions north of the African easterly jet (AEJ).

This work also suggests that the quality of the ECMWF reanalysis is sufficient to realistically represent the main characteristics of the flow circulation over the west Africa, allowing to initialise Meso-NH at high resolution. Nevertheless the weak points are the humidity field and the soil water content that are crucial for further development of convection. In general a moist bias is noted, especially north of the AEJ as compared with available observations. It should be also noticed that budgets are available from these simulations, that have been performed to test and improve single column models over that region in the frame of the WAMP.

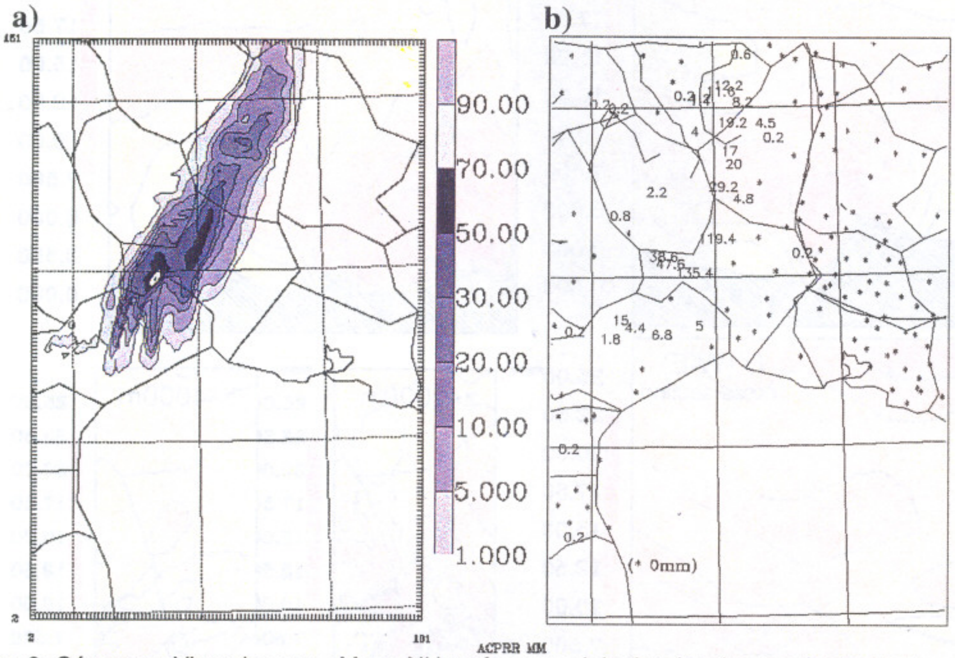


Figure 9: Cévennes-Vivarais case : Meso-NH surface precipitation (mm) accumulated between 01 UTC and 06 UTC (a) as compared with the surface mesonet observations (b).

## 3. Conclusion

We illustrated here the benefit brought by high resolution simulations. Whereas the gain is weak but sensible for strong forced cases, it becomes strong for intense convective cases especially in the tropical and equatorial regions. Resolutions equal or less that 5 km allow an explicit representation of convection, that conveniently can avoid the use of a convective scheme.

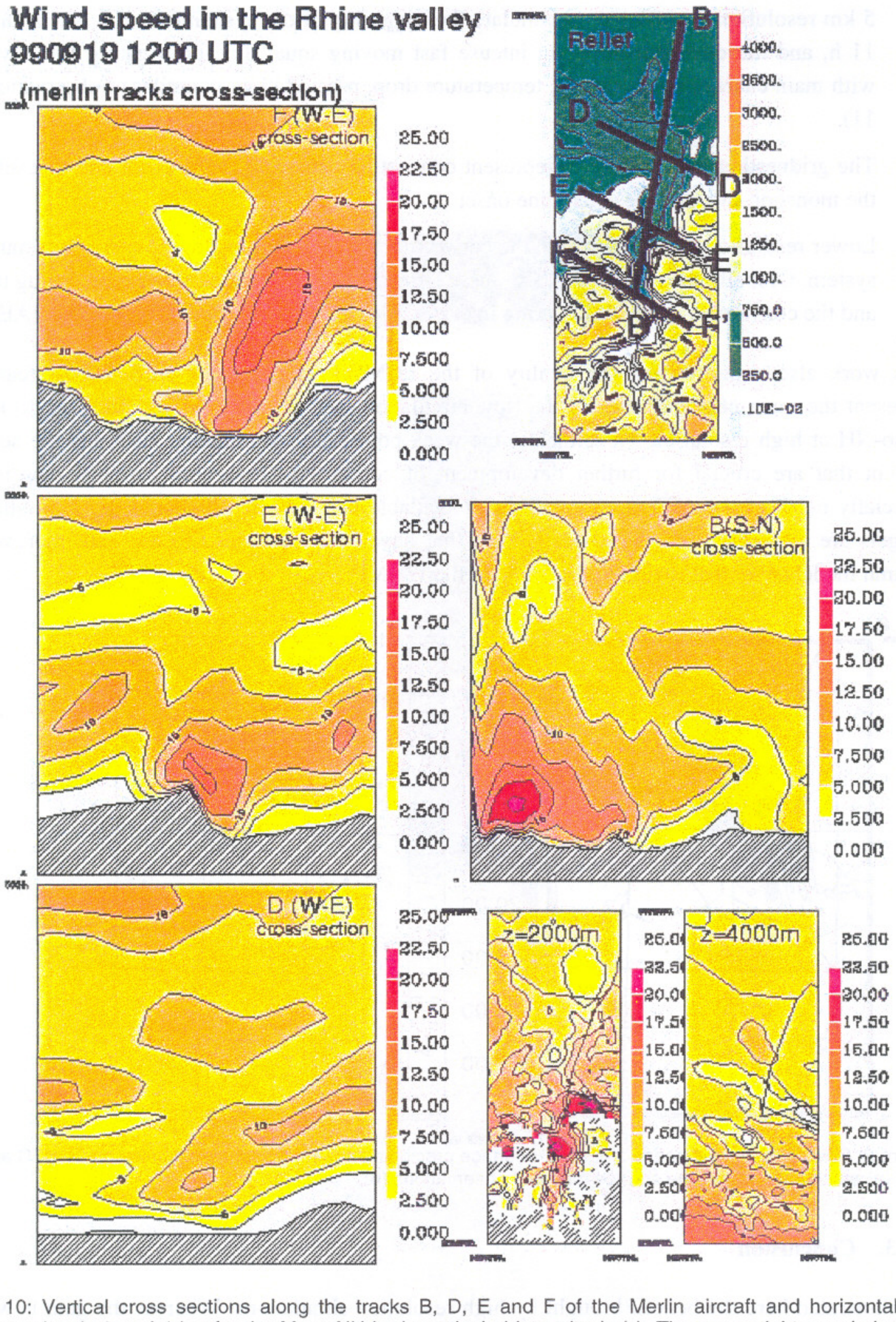


Figure 10: Vertical cross sections along the tracks B, D, E and F of the Merlin aircraft and horizontal cross sections at levels 2 and 4 km for the Meso-NH horizontal wind intensity (m/s). The upper right panel shows the Merlin horizontal trajectory superposed to the Rhine valley topography.

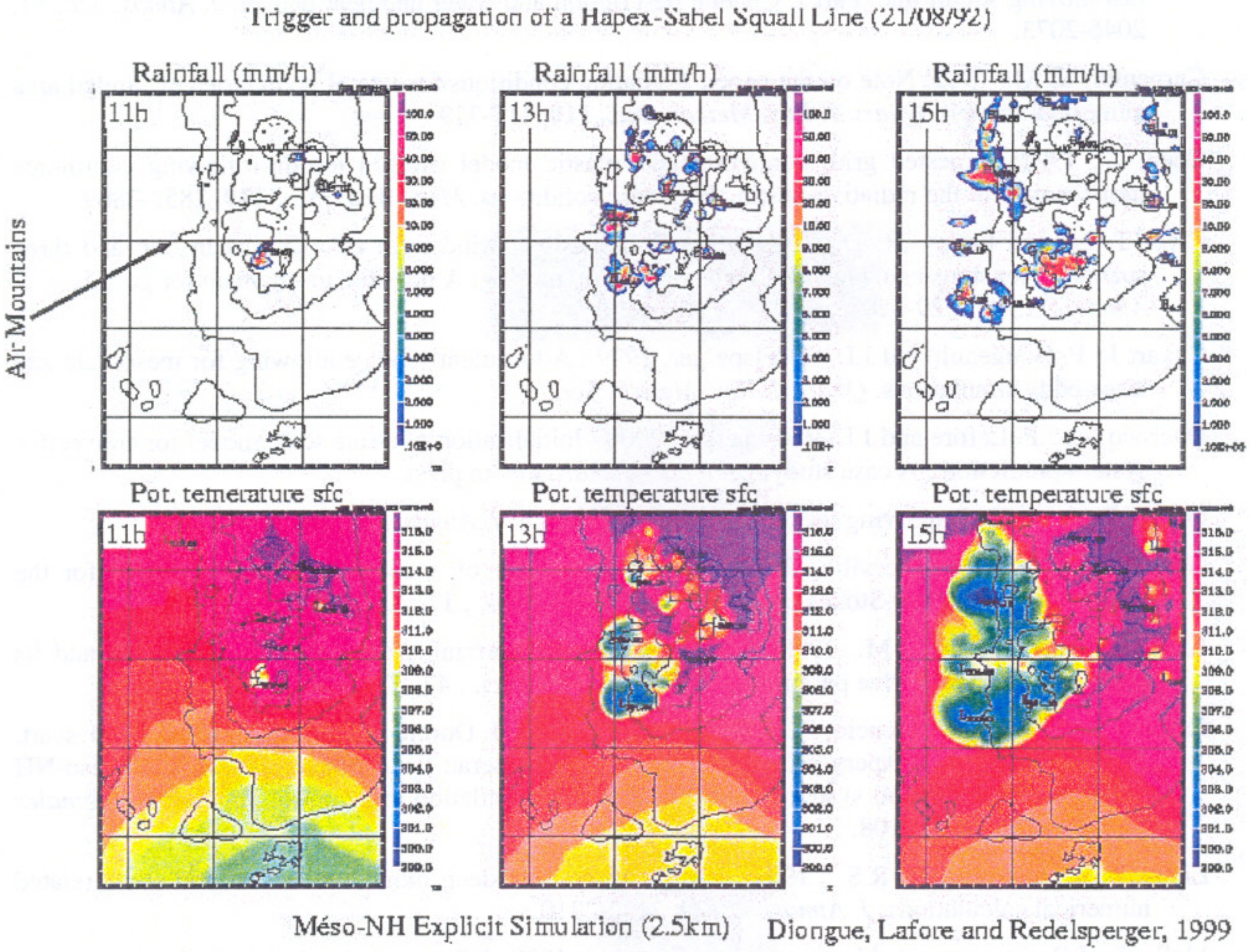


Figure 11: Evolution of the surface rain rate (mm/hr) and surface temperature (1°C isoline interval) simulated by Meso-NH at 11h, 13h and 15h.

Outside progresses to be done to increase the efficiency of numerical schemes at small scales, the improvement of the humidity field at those scales appears as a priority to release the potential benefit of high resolution simulations.

Finally owing to the gridnesting technique and powerful diagnostics, Meso-NH can contribute to develop and test new parametrisation schemes.

## 4. References

Bélair S., Lacarrère, P., Noilhan, J., Masson, V. and Stein, J., 1998: High-resolution simulation of surface and turbulent fluxes during HAPEX-MOBILHY. *Mon. Wea. Rev.*, **126**, 2234-2253.

Bechtold, P., Redelsperger, J. L., Beau, I. , Blackburn, M. , Brinkop, S., Grandpeix, J.Y., Grant, A., Gregory, D. , Guichard, F., Hoff,C. and Ionnidou, E., 1998: A GCSS model intercomparison for a tropical squall line observed during TOGA-COARE. Part II: Intercomparison of SCMs with a CRM. *Quart. J. Roy. Meteor. Soc.*

Bougeault P. and Lacarrère, P., 1989: Parameterization of orography-induced turbulence in a meso-beta-scale model. *Mon. Wea. Rev.*, **117**, 1872-1890.

Caniaux, G., J.L. Redelsperger, and J.P. Lafore, 1994: A numerical study on the stratiform region of a fast moving squall line. Part I: General description and water and heat budget. *J. Atmos. Sci.*, **51**, 2046-2073.

Carpenter, K. M., 1982: Note on the paper: Radiation conditions for lateral boundaries of limited area numerical models. *Quart. J. Roy. Meteor. Soc.*, **110**, 717-719.

Chen, C., 1991: A nested grid, nonhydrostatic, elastic model using a terrain-following coordinate transformation: the radiative-nesting boundary conditions. *Mon. Wea. Rev.,* **119**, 2852-2869.

Clark T. L., and Farley ,R. D. , 1984: Severe downslope windstorm calculations in two and three spatial dimensions using anelastic interactive grid nesting: A possible mechanism for gustiness. *J. Atmos. Sci.,* 41, 329-350.

Cuxart J., P. Bougeault and J.L. Redelsperger, 1999 : A turbulent scheme allowing for mesoscale and large-eddy simulations. *Quart. J. Roy. Meteor. Soc.*,.

Ducrocq V., J.P. Lafore and J.L. Redesperger, 2000 : Initialisation of a fine scale model for convective system prediction : A case study. *Quart. J. Meteor. Soc.* in press.

Durran D. R., 1989: Improving the anelastic approximation. *J. Atmos. Sci.*, **46**, 1453-1461.

Gal-Chen, T., and Sommerville, R.C.J., 1975: On the use of a coordinate transformation for the solution of the Navier-Stokes equations. *J. Comput. Phys.* , **17**, 209-228.

Kain, J.S. and Fritsch, J. M., 1990: A one-dimensional entraining/detraining plume model and its application in convective parameterizations. *J. Atmos. Sci.* , **47**, 2784-2802.

Lafore J.P., J. Stein, N. Asencio, P. Bougeault, V. Ducrocq, J. Duron, C. Fisher, P. Héreil, P. Mascart, J.P. Pinty, J.P. Redelsperger, E. Richard, and Vilà-Guerau de Arellano, 1998 : The Méso-NH atmospheric simulation system. Part I : Adiabatic formulation and control simulations. *Annales Geophysicae*, **16**, 90-108.

Lipps, F. B., and Hemler, R.S. , 1982: A scale analysis of deep moist convection and some related numerical calculations. *J. Atmos. Sci,* 39, 2192-2210.

Mallet I., J.P. Cammas, P. Mascart and P. Bechtold, 1999: Effects of cloud diabatic heating on the early development of the FASTEX IOP17 cyclone. *Quart. J. Meteor. Soc.*, **125**, 3439-3468.

Morcrette, J. 1989: Description of the radiation scheme in the ECMWF model. *ECMWF Tech. Memo.* **165**, 872-886.

Nuret M., M. Chong, J.P. Lafore, O. Bousquet and V. Gouget, 2000 : On the impact of Doppler radar-derived wind fields in a mesoscale non-hydrostatic model. *Quart. J. Meteor. Soc.* in press.

Pinty J.P. and P. Jabouille, 1998 : A mixed-phased cloud parameterization for use in a mesoscale non-hydrostatic model : simulation of a squall line and of orographic precipitations. *In Conf. on Cloud Physics,* page 217-220, Everett, WA. Amer. Meteor. Soc.

Redelsperger, J.-L., and G. Sommeria, 1986: Three-dimensional simulation of a convective storm: Sensitivity studies on subgrid parameterization and spatial resolution. *J. Atmos. Sci.*, **43**, 2619-2635.

Stein J., E. Richard, J.P. Pinty, N. Asencio et S. Cosma, **2000 :** High-Resolution Non-Hydrostatic Simulations of Flash-Flood Episodes with grid-nesting and ice-phase parameterization, *Meteor. Atmos. Physics*, 72 : 203-221.

Viviand, H., 1974: Formes conservatives des 'equations de la dynamique des gaz. *Rech. Aérosp.,* **1**, 65-66.

Wilhelmson, R., and Y. Ogura, 1972: The pressure perturbation and the numerical modeling of a cloud. *J. Atmos. Sci.*, **29**, 1295-1307.